

# Projection-Based Denoising Method for Photon-Counting Energy-Resolving Detectors

Yanye Lu<sup>1,5</sup>, Michael Manhart<sup>1,3</sup>, Oliver Taubmann<sup>1,4</sup>, Tobias Zobel<sup>1</sup>, Qiao Yang<sup>1</sup>, Jang-hwan Choi<sup>2</sup>, Meng Wu<sup>2</sup>, Arnd Doerfler<sup>3</sup>, Rebecca Fahrig<sup>2</sup>, Qiushi Ren<sup>5</sup>, Joachim Hornegger<sup>1,4</sup>, Andreas Maier<sup>1,4</sup>

<sup>1</sup>Pattern Recognition Lab, Department of Computer Science, Friedrich-Alexander-Universität Erlangen-Nürnberg, Germany

<sup>2</sup>Department of Radiology, Stanford University, CA, USA

<sup>3</sup>Department of Neuroradiology, Universitätsklinikum Erlangen, Germany

<sup>4</sup>Erlangen Graduate School in Advanced Optical Technologies (SAOT), Germany

<sup>5</sup>Department of Biomedical Engineering, Peking University, Beijing, China

yan.ye.lu@fau.de

**Abstract.** In this paper, we present a novel projection-based novel noise reduction method for photon counting energy resolving detectors in Spectral Computed Tomography (CT) imaging. In order to denoise the projection data, a guidance image from all energy channels is computed, which employs a variant of the joint bilateral filter to denoise each energy bin individually. The method is evaluated by a simulation study of cone beam CT data. We achieve a reduction of noise in individual channels by 80% while at the same time preserving edges and structures well in the results, which indicate that the methods are applicable to clinical practice.

## 1 Introduction

Polychromatic X-ray sources are commonly employed for medical Computed Tomography (CT). However, most of them are processed as mono-energetic CT measurements by conventional CT detectors which can not take advantage of the energy information in the X-ray beam. In recent years, development of Spectral Computed Tomography (SCT), which plays a vital role in Quantitative Computed Tomography (QCT) [1], has been accelerated by many technologies in both hardware and software. For QCT-reconstruction, spectral input data requires multiple measurements with different spectral characteristics of each projection bin. SCT facilitates the quantitative measurement of material properties. It has broad potential for applications in the preclinical and the clinical field, allowing for visualization of bone and plaque, measurement of blood volume, or quantification of contrast agent concentrations.

Unfortunately, by splitting the acquired photons into different energy bins, each energy channel suffers from a low signal-to-noise ratio leading to noisy projection images, especially in the low energy portion of the energy spectrum. Therefore an appropriate noise reduction method is required to obtain reliable

image quality in clinical applications. Iterative reconstruction methods have shown superior advantages in noise reduction, but suffer from high complexity, which is a shortcoming in practical applications, especially in interventional medical image processing cases. It is worth mentioning that the noise from photon-counting energy-resolving detectors can be modeled by using Poisson statistics accurately and easily, which is a great advantage in projection based denoising processing. In light of this, besides post-processing approaches on reconstructed images, filtering in pre-processing on projection data is also presented by several studies, such as using noise adaptive filter kernels [2, 3] and edge preserving filters [4, 5].

In this paper, we present a novel contribution to bring this new technology closer to clinical practice: improved noise reduction using non-linear techniques in fluoroscopic imaging. Below we give a short review of X-ray absorption physics, then describe our denoising approach. Subsequently, simulated results are presented.

## 2 Materials and methods

### 2.1 Polychromatic X-ray absorption

Traditional X-ray detectors measure the integral of the incident X-ray spectrum at each pixel

$$I = \sum_{i=1}^E N_i L_i e^{-\sum_{j=1}^M \mu_{ij} l_j} \quad (1)$$

where  $E$  denotes the number of considered energy levels,  $N_i$  the number of emitted photons at energy level  $L_i$ ,  $M$  the number of considered materials,  $\mu_{ij}$  the energy and material dependent X-ray absorption, and  $l_j$  the path length in the respective material  $j$ . In this measurement, each photon is weighted with its energy, which results in a weighted sum of Poisson distributed random variables.

Photon-counting detectors are able to detect each photon individually. Thus, the integral from (1) simplifies to

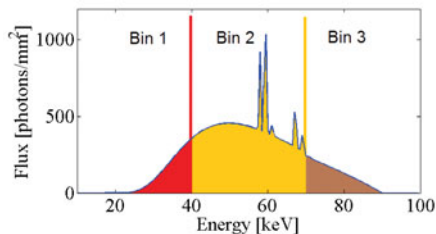


**Fig. 1.** Binning of a X-ray spectrum into 3 bins.

$$I = \sum_{i=1}^E N_i e^{-\sum_{j=1}^M \mu_{ij} l_j} \quad (2)$$

In the energy-resolving case, we get more than a single measurement per pixel (Fig. 1). We differentiate the photons into  $b = 1 \dots B$  different energy channels or bins

$$I_b = \sum_{i=l_b^s}^{l_b^e} N_i e^{-\sum_{j=1}^M \mu_{ij} l_j} \quad (3)$$

where  $l_b^s$  and  $l_b^e$  are the respective start and end indices of the considered energies in bin  $b$ . The energy-selective channels suffer from more noise than the measurements over the complete spectrum, because number of photons corresponding to each bin is reduced from  $I_0 = \sum_{i=0}^{E-1} N_i$  to  $I_b^0 = \sum_{i=l_b^s}^{l_b^e} N_i$  and the signal-to-noise ratio in the Poisson process is proportional to  $\sqrt{I_0}$  and  $\sqrt{I_b^0}$ , respectively.

## 2.2 Noise reduction with joint bilateral filtering

To obtain an image with distinct structures and reduced noise, we add the photons of all energy-selective projection images  $I_b$  to recover the projection image  $I$  covering the full energy spectrum

$$I = \sum_{b=1}^B I_b \quad (4)$$

Note that this procedure is optimal in terms of weighting of the noise variances. We use  $I$  as a guidance image for a joint bilateral filter (JBF) [6] to compute energy-selective projection images  $I'_b$  with reduced noise but preserved structures

$$I'_b(x, y) = \frac{1}{c(x, y)} \sum_{i, j} g_s(x, i, y, j) g_I(x, i, y, j) I_b(x, y) \quad (5)$$

$$c(x, y) = \sum_{i, j} g_s(x, i, y, j) g_I(x, i, y, j) \quad (6)$$

$$g_s(x, i, y, j) = e^{-\frac{(x-i)^2 + (y-j)^2}{2\sigma_s}} \quad (7)$$

$$g_I(x, i, y, j) = e^{-\frac{(I(x, y) - I(i, j))^2}{2\sigma_I}} \quad (8)$$

where  $g_s(x, i, y, j)$  is the spatial kernel controlled by  $\sigma_s$  and  $g_I(x, i, y, j)$  is the range kernel controlled by  $\sigma_I$  and the guidance image  $I$ .

The range kernel is configured such that a certain contrast difference  $D$  is preserved

$$D = I_1 - I_2 \quad (9)$$

In case of a monochromatic angiography image,  $D$  can be defined using  $I_1 = I^0 e^{-\mu^{\text{bg}} l^{\text{bg}}}$  and  $I_2 = I^0 e^{-(\mu^{\text{bg}} l^{\text{bg}}) - (\mu^{\text{v}} l^{\text{v}})}$ . The X-ray absorption  $\mu^{\text{bg}}$  and the path length  $l^{\text{bg}}$  correspond to the anatomic background, while  $\mu^{\text{v}}$  and  $l^{\text{v}}$  define absorption and path length corresponding to a contrast agent filled vessel. Insertion into (9) yields

$$D = I_1 - I_2 = I^0 e^{-\mu^{\text{bg}} l^{\text{bg}}} - I^0 e^{-(\mu^{\text{bg}} l^{\text{bg}}) - (\mu^{\text{v}} l^{\text{v}})} = I_1 (1 - e^{-\mu^{\text{v}} l^{\text{v}}}) = I_1 z \quad (10)$$

where the parameter  $z$  is only dependent on the vessel size and material. Note that  $z$  can be conveniently computed as  $z = 1 - \frac{I_2}{I_1}$ . This leads to a contour adaptive definition of the bilateral filter with  $\sigma_I = \bar{I}(x, y) \cdot z$ , where  $\bar{I}(x, y)$  is the mean value of the guidance image in a local neighborhood.

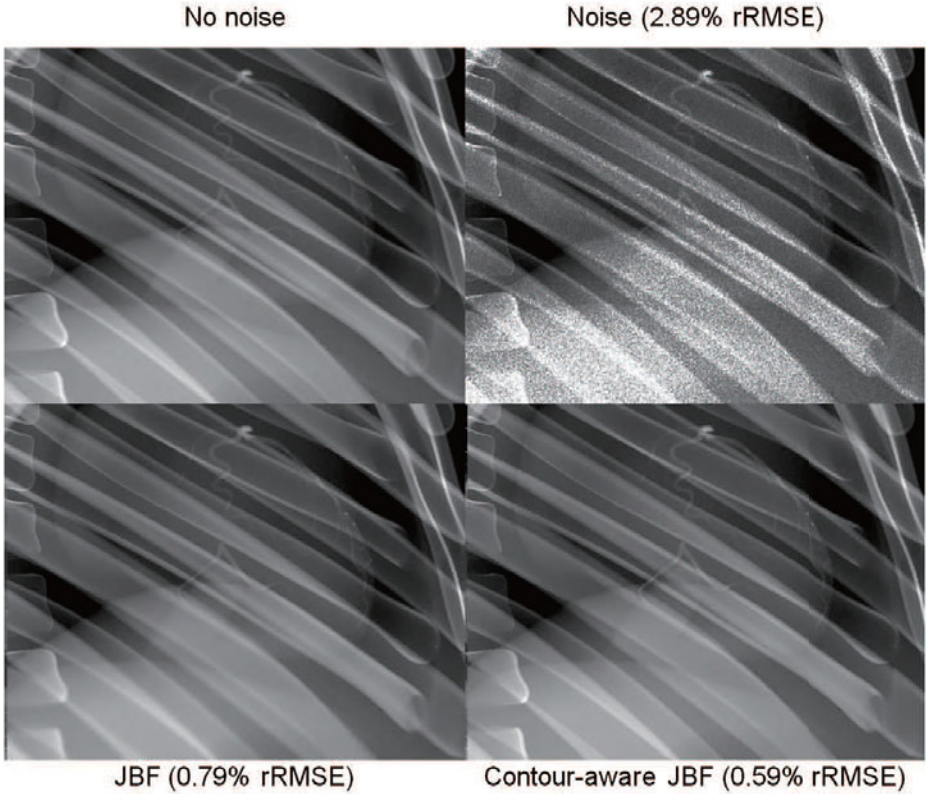


**Fig. 2.** Line integral images with and without noise (top row) and after restoration using JBF filtering (bottom row).

## 2.3 Experimental setup

We simulated a set of fluoroscopic images using an append buffer based rendering procedure [7] using XCAT [8]. An X-ray spectrum with the same half layer values as a commercially available C-arm system is used. Projection size was simulated with  $620 \times 480$  pixels with a pixel size of  $0.6 \times 0.6$  mm. The peak-voltage was set to 90 kV. We applied a time current product of 2.5 mAs, which is comparable to the dose setting per projection in a clinical 3D scan. The projection was centered around the heart to focus on the coronary arteries, which were filled with an iodine-based contrast medium (comparable to Ultravist 370). Energy-dependent X-ray absorption coefficients for elemental data and compounds such as bone were obtained from the NIST database [9]. All methods were implemented in the CONRAD framework [10] and will be made available as open source software.

## 3 Results

Fig. 2 displays the simulated images of the first energy channel with and without noise. The relative root mean square error (rRMSE) that is normalized with the maximal intensity in the noise-free image is reduced from 2.89% to 0.59%. Note that the rRMSE was only evaluated at pixels that did not suffer from photon starvation (excessive white noise) in the noisy image, while all pixels were considered for the JBF denoised images.

## 4 Discussion

We presented a novel approach for noise reduction of energy-resolved projection images. The idea of a contour-aware joint bilateral filtering to energy-resolving detectors is applied in this study, which could reduce noise but well preserve edges and structures. As shown in the result, denoising with JBF and contour-aware JBF is very successful, which could reduce noise by 80% while at the same time preserving edges and structures well. We will apply this method to realistic data in the future work and explore potential clinical applications.

**Acknowledgement.** The authors gratefully acknowledge funding of the Medical Valley national leading edge cluster, Erlangen, Germany, diagnostic imaging network, sub-project BD 16, research grant nr. 13EX1212G.

## References

1. Heismann BJ, Schmidt BT, Flohr TG. Spectral computed tomography. Proc SPIE. 2012.
2. Kachelrieß M, Watzke O, Kalender WA. Generalized multi-dimensional adaptive filtering for conventional and spiral single-slice, multi-slice, and cone-beam CT. Med Phys. 2001;28(4):475–90.

3. Zeng GL, Zamyatin A. A filtered backprojection algorithm with ray-by-ray noise weighting. *Med Phys.* 2013;40(3):031113–1–7.
4. Manduca A, Yu L, Trzasko JD, et al. Projection space denoising with bilateral filtering and CT noise modeling for dose reduction in CT. *Med Phys.* 2009;36(11):4911–9.
5. Manhart M, Fahrig R, Hornegger J, et al. Guided noise reduction for spectral CT with energy-selective photon counting detectors. *Proc CT Meet.* 2014; p. 91–4.
6. Petschnigg G, Szeliski R, Agrawala M, et al. Digital photography with flash and no-flash image pairs. *ACM Trans Graph.* 2004;23(3):664–72.
7. Maier A, Hofmann HG, Schwemmer C, et al. Fast simulation of x-ray projections of spline-based surfaces using an append buffer. *Phys Med Biol.* 2012;57(19):6193–210.
8. Segars WP, Sturgeon G, Mendonca S, et al. 4D XCAT phantom for multimodality imaging research. *Med Phys.* 2010;37(9):4902–15.
9. Hubbell JH, Seltzer SM. Tables of X-ray Mass Attenuation Coefficients and Mass Energy Absorption Coefficients. National Inst. of Standards and Technology-PL, Gaithersburg, MD (United States). Ionizing Radiation Div.; 1995.
10. Maier A, Hofmann H, Berger M, et al. CONRAD: a software framework for cone-beam imaging in radiology. *Med Phys.* 2013;40(11):111914–1–8.